

SUPPLEMENTARY SUPPORTING INFORMATION

Effective Discrimination of GTP from ATP by a Cationic Tentacle Porphyrin through “Turn-On” Fluorescence Intensity

Suneesh C. Karunakaran,^a Albish K. Paul^a and Danaboyina Ramaiah^{a,b*}

^aPhotosciences and Photonics, Chemical Sciences and Technology Division, CSIR-National Institute for Interdisciplinary Science and Technology, Trivandrum 695 019, India

^bCSIR-North East Institute of Science and Technology, Jorhat - 785 006, Assam, India

E-mail: rama@niist.res.in, d.ramaiah@gmail.com

S. No.		Page
1	Experimental section	2
2	Fig. S1 shows the normalized absorption and fluorescence spectra of PyP and its zinc complex Zn-PyP .	5
3	Fig. S2 shows the changes in absorption and emission spectra of the porphyrin derivative PyP with the successive addition of GDP in phosphate buffer.	5
4	Fig. S3 shows the changes in absorption and emission spectra of the porphyrin derivative PyP with the successive addition of GMP in phosphate buffer.	6
5	Fig. S4 shows the changes in absorption and emission spectra of the porphyrin derivative PyP with the successive addition of ATP in phosphate buffer.	6
6	Fig. S5 Relative changes in the absorbance of Zn-PyP in the presence of various nucleotides.	7
7	Fig. S6 shows the relative changes in absorbance of PyP with GTP at various ionic strengths in 10 mM phosphate buffer.	7
8	Fig. S7 shows the relative fluorescence quenching of HPTS by the cationic porphyrin PyP in 10 mM phosphate buffer at various ionic strengths.	8
9	Fig. S8 shows the linear plot of the fluorescence enhancement of [PyP -HPTS] upon gradual addition of GTP for the estimation of limit of detection.	8
10	Fig. S9 shows the relative concentration dependent enhancement of fluorescence intensity of [PyP •HPTS] and [Zn-PyP •HPTS] complexes by various nucleotides in phosphate buffer.	9
11	Fig. S10 shows the fluorescence decay profiles of HPTS and the complex [PyP •HPTS] in the absence and presence of GTP, collected at 515 nm.	9

EXPERIMENTAL SECTION

General experimental techniques. The equipment and procedures for melting point determination and spectral recordings have been described elsewhere.^{1,2} ^1H and ^{13}C NMR spectra were measured on a 300 or 500 MHz Bruker advanced DPX spectrometer. The electronic absorption spectra were recorded on a Shimadzu UV-VIS-NIR spectrophotometer. Fluorescence spectra were recorded on a SPEX-Fluorolog F112X spectrofluorimeter. MALDI-TOF MS analysis was performed with a Shimadzu Biotech Axima CFRplus instrument equipped with a nitrogen laser in the linear mode using 2,5-dihydroxybenzoic acid (DHB) as the matrix. Fluorescence lifetimes were measured using IBH (FluoroCube) time-correlated picosecond single photon counting (TCSPC) system. The samples were excited with a pulsed diode laser (<100 ps pulse duration) at 375 nm (NanoLED-11) with a repetition rate of 1 MHz. The detection system consisted of a microchannel plate photomultiplier (5000U-09B, Hamamatsu) with a 38.6 ps response time coupled to a monochromator (5000M) and TCSPC electronics [data station Hub including Hub-NL, NanoLED controller, and preinstalled fluorescence measurement and analysis studio (FMAS) software]. The fluorescence decay profiles were deconvoluted using IBH data station software V2.1 and minimizing the χ^2 values of the fit to 1 ± 0.1 . All experiments were carried out at room temperature (25 ± 1 °C), unless otherwise mentioned.

Materials. The chemicals and reagents used in the study were purchased from SD Fine Chemicals, India; Sigma-Aldrich; U.S.A. Merck Chemicals, Germany and were used as such without further purifications. The standard Tetraphenyl porphyrin (TPP) was synthesized according to modified Lindsey's method.³ The cationic porphyrin PyP was synthesized by the reported procedure.⁴

Synthesis of 5,10,15,20-tetrakis[4-(8-bromooctyloxy)phenyl]porphyrinato zinc (II). A solution of the 5,10,15,20-tetrakis[4-(8-bromooctyloxy)phenyl]porphyrin (0.14 mmol) in a mixture (1:2) of methanol and chloroform (25 mL) was stirred with zinc acetate (0.7 mmol) for 6 h at 25 °C. The completion of reaction was monitored through absorption changes using a UV-vis spectrometer. The solvent was distilled off under

reduced pressure and the residue obtained was chromatographed over silica gel using dichloromethane as the eluent to give the starting bromoporphyrin derivative.

Yield: (95%). mp > 300 °C; ¹H NMR (500 MHz, CDCl₃, 30 °C, TMS): δ 1.469-1.541 (m, 24 H), 1.627 (s, 8 H), 1.926-1.993 (m, 16H), 3.462 (t, 8 H, J=7 Hz), 4.222 (t, 8 H, J=6 Hz), 7.252 (d, 8 H, J=8.5 Hz), 8.113 (8 H, J=8 Hz), 8.992 (s, 8 H); ¹³C NMR (125 MHz, CDCl₃, 30 °C, TMS): δ 26.16, 28.16, 28.79, 29.33, 29.47, 32.85, 34.07, 68.21, 112.57, 120.80, 131.88, 136.11, 135.40, 150.49, 158.73; MALDI-TOF-MS: m/z Calcd for C₇₉H₉₇Br₄N₄O₄Zn: 1551.69; Found 1553.65 (M+2)⁺.

Synthesis of 5,10,15,20-Tetrakis[4-(8-pyridiniooctyloxy)phenyl]porphyrinato zinc(II) tetrabromide (Zn-PyP). 5,10,15,20-tetrakis[4-(8-bromooctyloxy)phenyl]-porphyrinato zinc(II) (0.13 mmol) was dissolved in 2 mL of dry pyridine and heated at 100 °C for 8 h. Excess pyridine was removed under reduced pressure. The residue obtained was dissolved in water, filtered and the saturated solution of NH₄PF₆ was added to precipitate the PF₆ salt of the porphyrin derivative. The PF₆ salt was then dissolved in acetonitrile and a saturated solution of tetrabutylammonium bromide was added to give the complex **Zn-PyP**.

Yield: (60%). mp > 300 °C; ¹H NMR (500 MHz, CD₃CN, 30 °C, TMS): (δ) 1.348 (s (broad), 24H), 1.483 (s, 8H), 1.803 (m, 8H), 1.904 (m, 8H), 4.073 (t, 8H, J=6.5 Hz), 4.387 (t, 8H, J=7.5 Hz), 7.140 (d, 8H, J=8.5 Hz), 7.929 (dd, 16H, J=6.5 Hz), 8.410 (t, 4H, (d, 8H, J=6 Hz), 8.821 (s, 8H); ¹³C NMR (125 MHz, CD₃CN, 30 °C, TMS): δ 30.83, 31.00, 33.85, 34.13, 34.37, 36.14, 67.08, 117.76, 125.65, 133.58, 140.46, 150.46, 150.92, 155.41, 164.05; MALDI-TOF-MS: m/z calcd for C₉₉H₁₁₇F₂₄N₈O₄P₄Zn: 2128.39; found 2130.37 (M+2)⁺.

Calculation of K_{ass} of porphyrin nucleotide interaction. Nucleotides, nucleosides and other analyte solutions were prepared in distilled water. The binding constants of the cationic porphyrin **PyP** with nucleotides were calculated using Benesi-Hildebrand equation (eq. 1).

$$\frac{1}{A_f - A_{ob}} = \frac{1}{A_f - A_{fc}} + \frac{1}{K(A_f - A_{fc})[\text{Ligand}]} \quad \text{eq. 1}$$

wherein, K is the equilibrium constant, A_f is the absorbance of free host, A_{ob} is the observed absorbance in the presence of various ligands and A_{fc} is the absorbance at saturation. The linear dependence of $1/(A_f - A_{ob})$ on the reciprocal of the ligand concentration indicates the formation of a 1:1 molecular complex between ligands and the host.

References

1. K. T. Arun, D. T. Jayaram, R. R. Avirah and D. Ramaiah, *J. Phys. Chem. B* 2011, **115**, 7122-7128.
2. V. S. Jisha, K. T. Arun, M. Hariharan and D. Ramaiah, *J. Phys. Chem. B* 2010, **114**, 5912-5919.
3. J. S. Lindsey, I. C. Schreiman, H. C. Hsu, P. C. Kearney and A. M. Marguerettaz, *J. Org. Chem.*, 1987, **52**, 827-836.
4. C. S. Prasanth, S. C. Karunakaran, A. K. Paul, V. Kussovski, V. Mantareva, D. Ramaiah, L. Selvaraj, I. Angelov, L. Avramov, K. Nandakumar and N. Subhash, *Photochem. Photobiol.* 2014, **90**, 628–640.

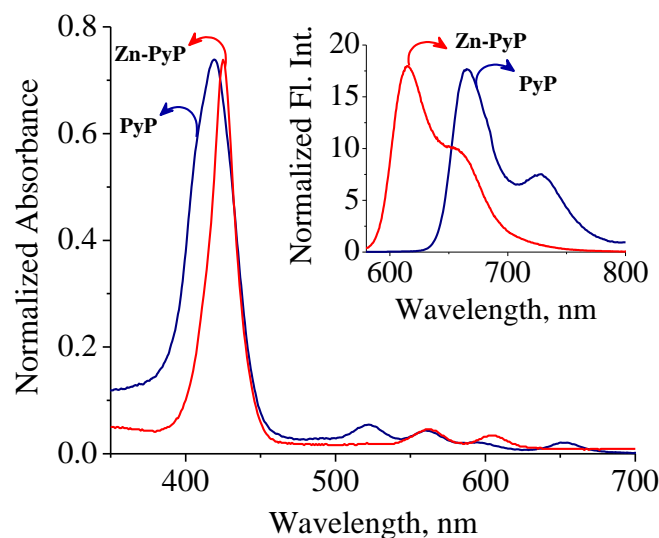


Figure S1. Normalized absorption and fluorescence (Inset) spectra of the pyridinium substituted cationic porphyrin **PyP** and its zinc complex **Zn-PyP** (4 μM) in water. λ_{ex} , 430 nm.

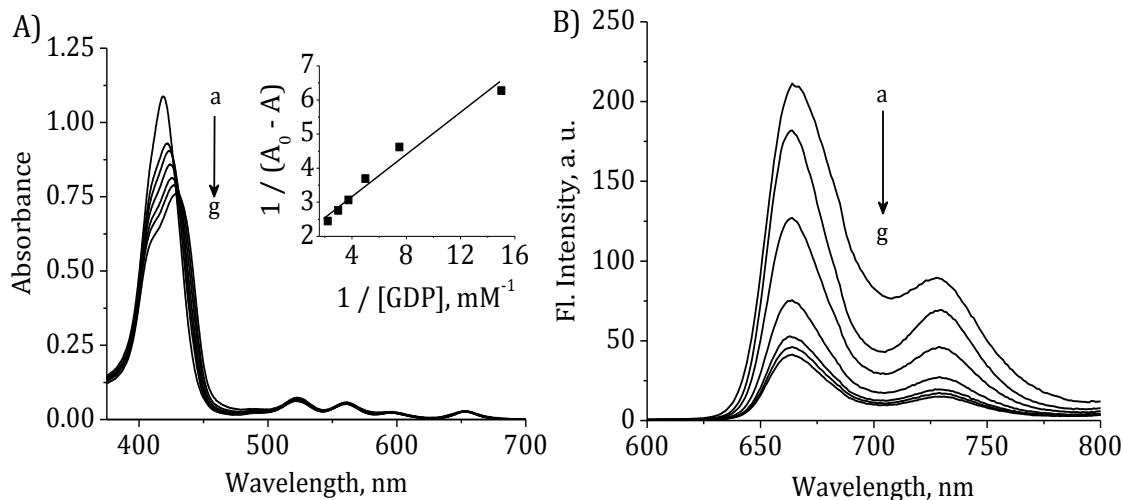


Figure S2. Changes in the (A) absorption and (B) emission spectra of the porphyrin derivative **PyP** (5 μM) with the successive addition of GDP in phosphate buffer (10 mM, pH 7.4). [GDP], (a) 0 and (g) 450 μM . Inset shows Benesi-Hildebrand plot for the binding of GDP with **PyP**. λ_{ex} , 430 nm.

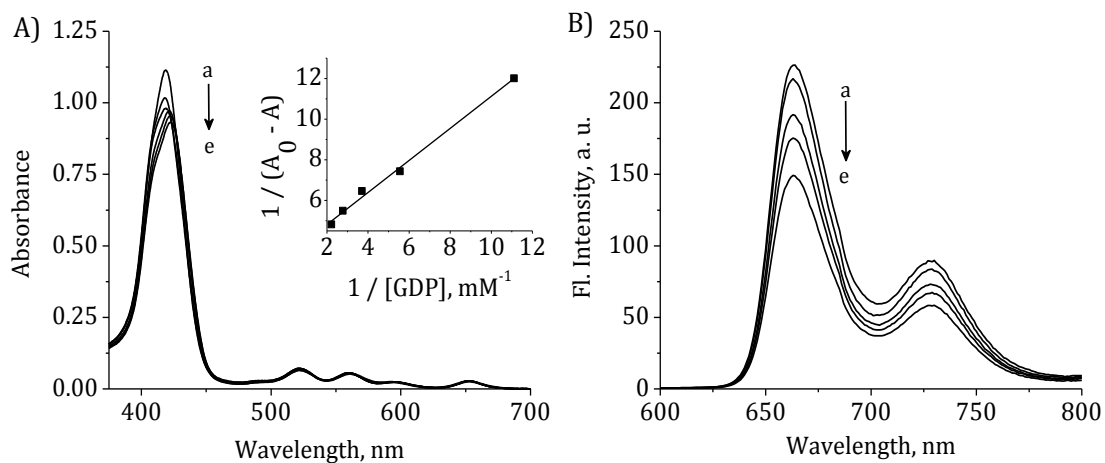


Figure S3. Changes in the (A) absorption and (B) emission spectra of the cationic porphyrin **PyP** (5 μM) with the successive addition of GMP in phosphate buffer (10 mM, pH 7.4). [GMP], (a) 0 and (e) 450 μM . Inset shows Benesi-Hildebrand plot for the binding of GMP with **PyP**. λ_{ex} , 430 nm.

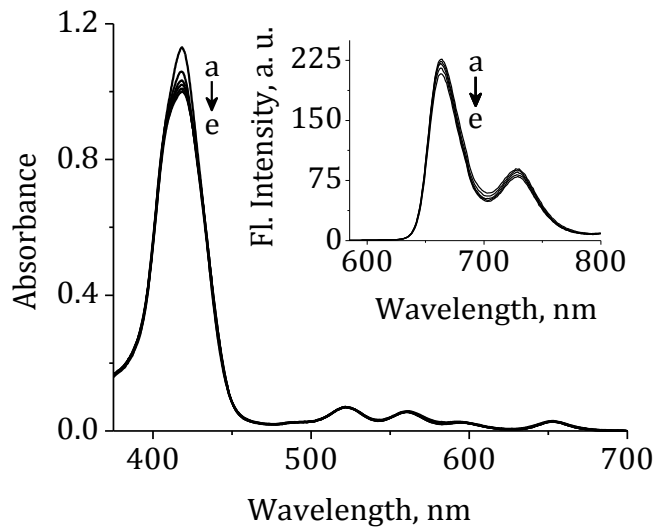


Figure S4. Changes in the absorption and emission (Inset) spectra of the porphyrin **PyP** (5 μM) with the addition of ADP in phosphate buffer (pH 7.4, 10 mM KH_2PO_4 , 2 mM NaCl). [ADP], (a) 0 and (e) 450 μM . λ_{ex} , 430 nm.

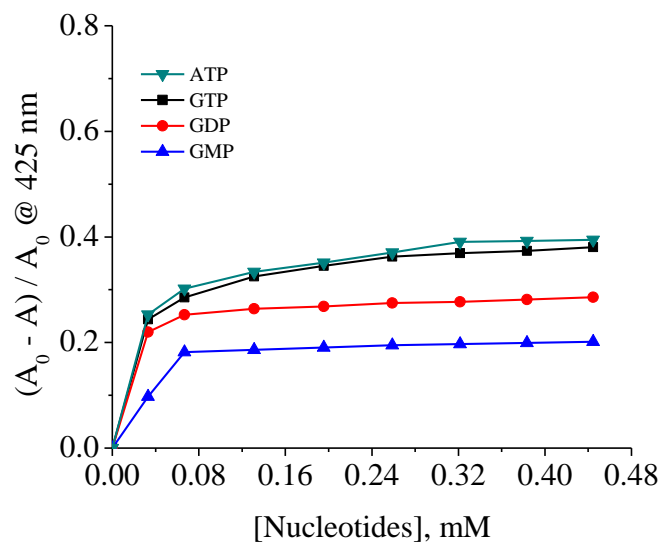


Figure S5. Relative changes in the absorbance of the zinc complex **Zn-PyP** (5 μ M) in the presence of various nucleotides.

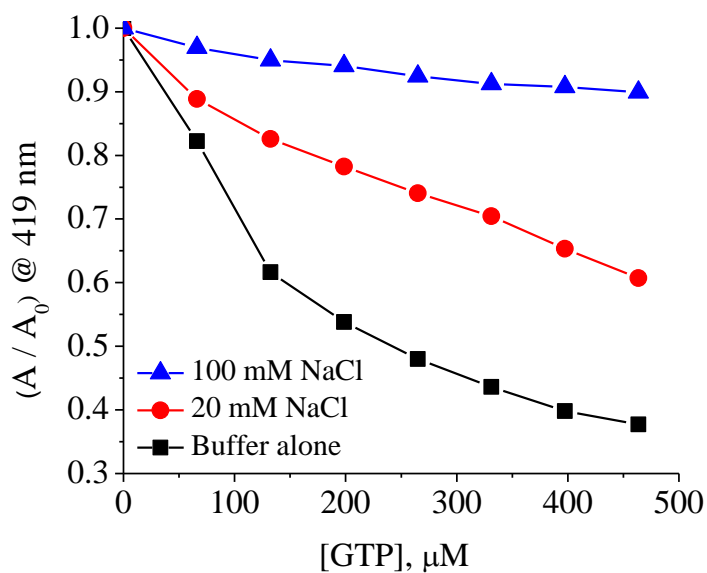


Figure S6. The relative changes in absorbance of **PyP** (5 μ M) with GTP (465 μ M) in 10 mM phosphate buffer (10 mM, pH 7.4) containing (■) 0, (●) 20, (▲) 100 mM NaCl.

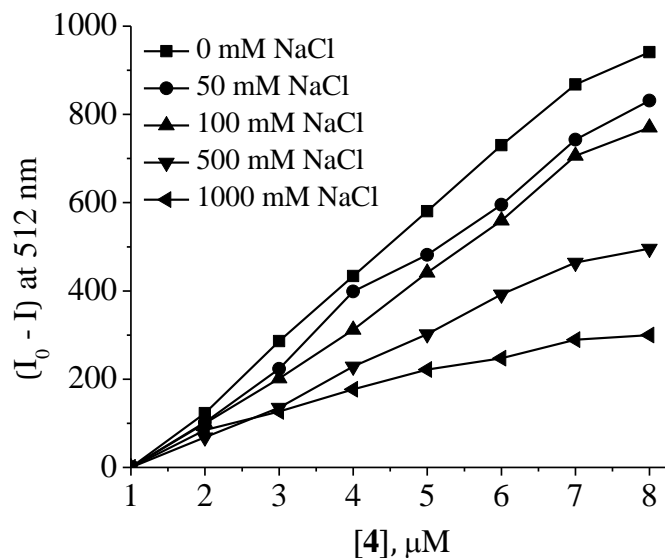


Figure S7. The relative fluorescence quenching of HPTS (4.5 μM) by the cationic porphyrin **PyP** (5.25 μM) in 10 mM phosphate buffer (10 mM, pH 7.4) containing (■) 0, (●) 50, (▲) 100 and (▼) 500 mM and (◄) 1M NaCl.

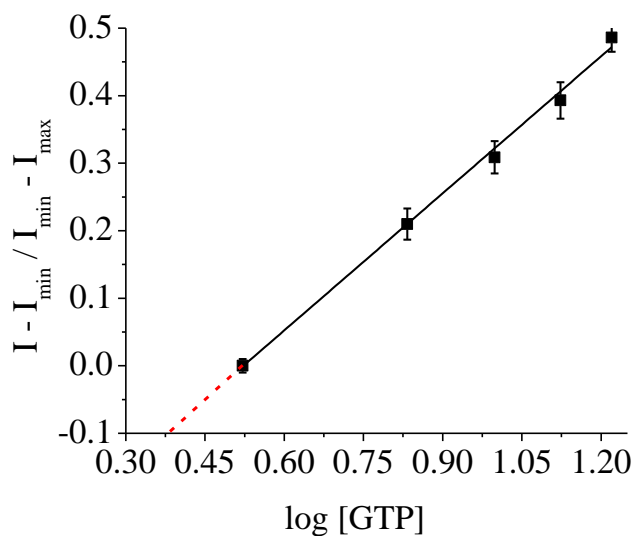


Figure S8. Linear plot of the fluorescence enhancement of [**PyP**-HPTS] upon gradual addition of GTP for the estimation of limit of detection. Data points represent the mean of more than three independent experiments.

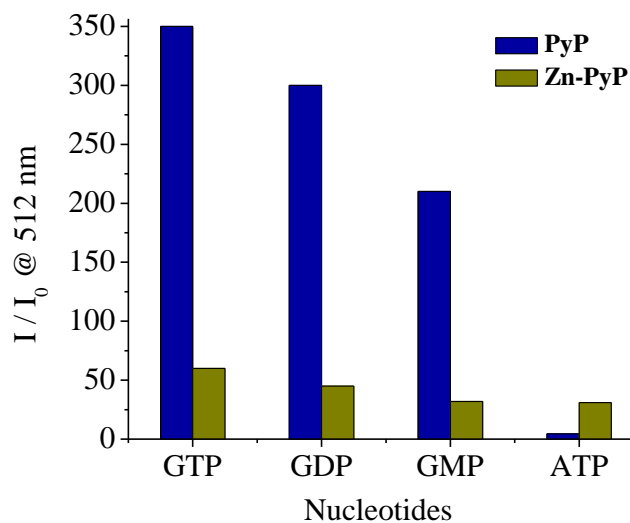


Figure S9. Relative concentration dependent enhancement of fluorescence intensity of [PyP•HPTS] and [Zn-PyP•HPTS] complexes by various nucleotides in phosphate buffer (10 mM, pH 7.4).

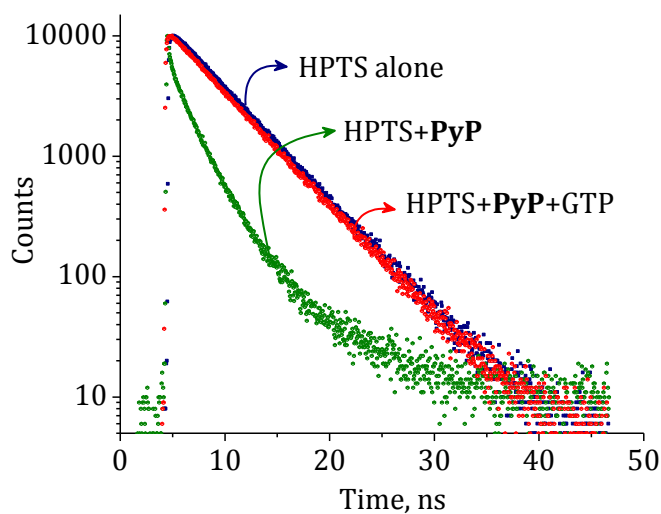


Figure S10. Fluorescence decay profiles of HPTS (4.5 μM) and the complex [PyP•HPTS] in the absence and presence of GT, collected at 515 nm. [PyP] 5.25 μM . λ_{ex} , 375 nm.